LAWRENCE
LIVERMORE
NATIONAL
LABORATORY

LLNL-JRNL-493145

Event Discrimination Using Regional Moment Tensors with Teleseismic-P Constraints

S. R. Ford, W. R. Walter, D. S. Dreger

August 12, 2011

Bulletin of the Seismological Society of America

Disclaimer

This document was prepared as an account of work sponsored by an agency of the United States government. Neither the United States government nor Lawrence Livermore National Security, LLC, nor any of their employees makes any warranty, expressed or implied, or assumes any legal liability or responsibility for the accuracy, completeness, or usefulness of any information, apparatus, product, or process disclosed, or represents that its use would not infringe privately owned rights. Reference herein to any specific commercial product, process, or service by trade name, trademark, manufacturer, or otherwise does not necessarily constitute or imply its endorsement, recommendation, or favoring by the United States government or Lawrence Livermore National Security, LLC. The views and opinions of authors expressed herein do not necessarily state or reflect those of the United States government or Lawrence Livermore National Security, LLC, and shall not be used for advertising or product endorsement purposes.

Event discrimination using regional moment tensors with teleseismic-P constraints

Sean R. Ford[1], William R. Walter[1], and Douglas S. Dreger[2]
[1]Lawrence Livermore National Laboratory [2]Berkeley Seismological Laboratory

Determining whether a seismic event is an earthquake, explosion, collapse, or something more complex can be done using regional (Δ<13°) intermediate-period (T>10s) full waveform moment-tensors down to low magnitudes (M~3.5). The moment tensor results can be improved for sparse station configurations when teleseismic (Δ>30°) array-based short-period (T<1s) P constraints are added. The inclusion of teleseismic-P aids in event discrimination because it samples the lower region of the focal-sphere, a region that intermediate-period waveforms recorded at the surface have low-sensitivity for shallow event depths. The teleseismic-P constraint is particularly useful in reducing the trade-off between a shallow explosion and shallow volume-compensated linear-vector dipole with a vertical axis in compression (VCLVD-P). This trade-off can complicate discrimination. The teleseismic-P constraint is applied to the source-type analysis of the announced nuclear test of the Democratic People's Republic of Korea on 25 May 2009 resulting in greater confidence in a dominantly explosive solution.

1. Introduction

The elements of the seismic moment-tensor can be used to derive the source-type. Determination of the source-type and discrimination between explosion, collapse, and earthquake sources can aid in the understanding of deformation in a region and in nuclear explosion monitoring. *Ford et al.* [2009] calculated a seismic moment-tensor for the announced nuclear test of the Democratic People's Republic of Korea (DPRK) on 25 May (Memorial Day) 2009 using regionally-recorded (<1500km), intermediate-period (10-50s) waveforms. The source-type derived from the seismic moment-tensor was dominantly explosive. An earthquake source was highly unlikely due to the poor fit to the data for any double-couple, or earthquake-like, source. However, another source-type with very little explosive component fit the data almost equally as well as an explosion. This source is described as a compensated linear-vector dipole with a vertical axis in compression (VCLVD-P).

The similarity in data-fit between the dominantly VCLVD-P source and dominantly explosive source presents a problem in discrimination between these two source-types. The reason for this VCLVD-P/explosion ambiguity is that the regional-distance intermediate-period recordings of a shallow event are most sensitive to the isotropic tensile radiation pattern along the equator of the focal sphere, which produces Rayleigh waves with uniform source phase, and which does not generate Love waves. The pure explosion and VCLVD-P radiation patterns differ significantly for small takeoff angle, where waves leave the source near-vertically. Incorporation of additional data sensitive to this vertical region of the focal sphere would constrain the VCLVD-P/explosion trade-off. We propose to use teleseismic-P recordings to constrain the moment-tensor-derived source type because, due to the steep take-off angles, the teleseismic-P waves are sensitive to the

lower hemisphere of the focal sphere where they are in dilation for a VCLVD-P and in compression for an explosion.

The use of only teleseismic data to determine the source-type has more serious trade-offs in terms of explosion monitoring, where there is little discrimination between shallow reverse mechanism earthquakes, explosions, and VCLVD in tension. However, in the absence of regional data relative amplitudes of teleseismic body-waves offer some ability to determine source-type and this was the approach of *Clark and Pearce* [1988], *Pearce et al.* [1988], and *Rogers and Pearce* [1992]. The combined use of regional and teleseismic data to constrain the source-type was done qualitatively by *Bowers* [1997] to discriminate between a collapse, explosion, and earthquake in a South African mine, and by *Bowers and Walter* [2002] to discriminate between a collapse and an explosion for mine events in Völkershausen, Germany and Wyoming, USA. In those studies the teleseismic-P waveform was shown to be inconsistent with sources determined via regional waveform-fitting. We propose a similar approach here, but with a more quantitative component afforded by the use of a source-type plot [*Hudson et al.*, 1989] with application to the 2009 Memorial Day explosion in the DPRK.

2. Data

Details of the regional data employed in this study can be found in *Ford et al.* [2009] and are summarized here. Three component waveform data from Global Seismograph Network (GSN) and China Digital Seismograph Network (CDSN) stations MDJ, INCN, BJT and HIA along with station TJN from the Ocean Hemisphere Project Seismological Network (Figure 1) are instrument corrected, integrated to displacement, and band-pass filtered using an 6th order acausal Butterworth filter with corners at 10 and 50 s. The regional data are plotted in black in Figure 2a. Green's functions for stations MDJ, INCN, and TJN were computed (with the program FKRPROG [*Saikia*, 1994]) using the MDJ2 velocity model [*Ford et. al*., 2009], with an adjustment to the velocities for stations BJT and HIA due to their greater distance (>1000 km).

Teleseismic data from International Monitoring System seismic arrays (Figure 1) in Alice Springs, Australia (ASAR), Haidmühle, Germany (GERES), and Mina, USA (NVAR), are processed following *Selby* [2010], where the array beam, *b*, at data point *i* is given by

$$b_i = \frac{1}{K}\sum_{k=1}^{K} x_{ki}\,, \tag{1}$$

where K is the number of channels in the array and x_{ki} is the recording at channel k at data point i corrected with time delays to produce the maximum beam power [*Rost and Thomas*, 2002]. These arrays are selected in this feasibility test due to their high SNR and simple teleseismic-P, though the inclusion of more array data is certainly possible. The array beam is band-pass filtered using an 8th order acausal Butterworth filter with corners at 0.8 and 4.5 Hz. The teleseismic data are plotted in black in Figure 2b. Teleseismic-P wavetrain (P+pP) Green's functions are calculated (with the program hudson96 [*Herrmann*, 2002]

based on *Hudson* [1969]) for the ak135 velocity model and convolved with the array instrument response and an attenuation operator (t^*=0.6s). The attenuation operator is similar to that used by *Ni et al.* [2010], though *Der and Lees* [1985] (while using a similar t^* for Southwestern US) show that it is much lower for other parts of Europe. However, there is no difference in the results for changes in $t^* \pm 0.2$ s for the method employed in this study and described in the next section. The regional and teleseismic Green's functions assume a source depth of 600m. There is little sensitivity to this assumption for variations in depth of ± 1 km.

3. Method and Results

We start with a description of confidence in the regional moment-tensor-derived source-type called the Network Sensitivity Solution (NSS). The NSS takes into account the unique station distribution, frequency band, and signal-to-noise ratio of a given event scenario. Details of the NSS approach are described in *Ford et al.* [2010] and briefly summarized here. The NSS compares the fit between the observed and forward-predicted data according to source-type. Source-type is parameterized by T and k as described in *Hudson et al.* [1989]. T measures the ratio of the deviatoric eigenvalues of the moment-tensor and plots along the horizontal axis. k measures the relative amount of isotropic moment and plots along the vertical axis. The axes are then transformed under the assumption that the moment-tensor eigenvalues are a uniformly distributed parameter to produce the source-type plot.

Fit is quantified with variance reduction, VR, given by

$$VR = 100 \times \left(1 - \sum_i r_i^2 \Big/ \sum_i d_i^2\right), \tag{2}$$

where r is the residual between the data, d, and the forward-predicted synthetic, s, summed over all data points, i. The forward problem used to produce the synthetic is described in *Minson and Dreger* [2007] and *Herrmann and Hutchenson* [1993]. Synthetics are produced for a number of sources sampled from a uniform distribution of moment tensor eigenvalues and eigenvectors. The sample size in this study is 10^7, but this could be reduced by an order of magnitude with little loss in source-type resolution. The greatest VRs are then contoured on a source-type plot. An example of an NSS for the 2009 Memorial Day explosion in the DPRK is given in Figure 2c.

The NSS in Figure 2c presents the trade-off in fit between an explosion-like source and a CLVD-like source, where the high-VR region encompasses both areas on the source-type plot. We dispense with this trade-off via the inclusion of teleseismic-P data that sample the lower part of the focal sphere to which the regional intermediate period data are insensitive.

Absolute teleseismic-P amplitudes are difficult to accurately model due to site variability [*Butler and Ruff*, 1980; *Cormier*, 1987] and inexact knowledge of the source model [*Douglas*, 1992; *Douglas*, 1993; *Murphy*, 1993]. Therefore, instead of measuring the fit between the

observed and predicted waveform as is done in the case of the regional data, we simply compare the predicted teleseismic-*P* polarity as parameterized by $CC_{\text{Tele-P}}$. $CC_{\text{Tele-P}}$ is the normalized correlation coefficient, *CC*, at each lag τ between the observed array beam, *b*, and predicted data, *g*, aligned on the analyst P-pick, where *CC* is given by

$$CC_{j\tau} = \frac{\sum_{i=\tau}^{i=\tau+N-1} b_{ij} g_{ij}}{\sqrt{\sum_{i=\tau}^{i=\tau+N-1} b_{ij}^2 \sum_{i=\tau}^{i=\tau+N-1} g_{ij}^2}}, \tag{3}$$

at each array *j* for each data point *i* in a window *N* samples long, where *N* = 160 (4 sec window) and $CC_{\text{Tele-P}}$ is

$$CC_{\text{Tele-P}} = \frac{1}{M} \sum_{j=1}^{j=M} \max(CC_{j\tau}) \text{ for } -10 \le \tau \le 10, \tag{4}$$

which is the average of *M* arrays maximum *CC* for lags ±10 samples and therefore $-1 \le CC_{\text{Tele-P}} \le 1$. The lag bounds are chosen so that cycle-skipping is minimized since 10 samples is ¼ sec which is the dominant period in the filtered data. If $CC_{\text{Tele-P}}$ is positive then the *VR* as calculated with the regional data (VR_{Reg}) is maintained and if is negative than VR_{Reg} is set to zero, so the new *VR* is defined as

$$VR = \begin{cases} VR_{\text{Reg}} & \text{for } CC_{\text{Tele-P}} \ge 0 \\ 0 & \text{for } CC_{\text{Tele-P}} < 0 \end{cases} \tag{5}$$

This operation is applied to the data and a new NSS is produced and shown in Figure 2d. A much tighter *VR* contour is produced around the best-fit solution and much of the trade-off area near the CLVD region is zeroed out.

4. Discussion

It is instructive to look at the regional and teleseismic waveforms of some theoretical sources and their corresponding *VR* and $CC_{\text{Tele-P}}$ to understand how the teleseismic constraint relaxes the Explosion/VCLVD-P trade-off and improves confidence in a given source-type. Figure 2a shows five sources and their theoretical regional waveforms along with their theoretical teleseismic-P waveforms in Figure 2b. The best-fit full (6-degree) moment tensor solution obtained via inversion of the regional waveforms is given in cyan and labeled Full. As expected, it fits the regional waveforms well with a *VR* of 81%. The *VR* and its source-type parameters are plotted in Figure 2c. However, as discussed in *Ford et al.* [2009], the best-fit deviatoric (5-degree) moment tensor solution shown in brown and labeled Dev has a *VR* of 80%. Both these solutions are far from a natural earthquake and one of the best-fit DC mechanisms is shown in purple and labeled DC2 where the fit to regional waveforms gives a VR of 72%. The contoured *VR* in the NSS shown in Figure 2c shows the separation between DC, near the center, and Explosion/CLVD, near the North and East edges, respectively. This separation is the basis for confidence in the

discrimination ability of the moment tensor approach. For comparison a pure explosion (1-degree) solution is shown in red and labeled Explosion, where the *VR* is 75%.

The best-DC presented in *Ford et al.* [2009] fit the data with a lower *VR* than the best-fit DC mechanism presented here, DC2. The discrepancy is due to different approaches used to find the best-fit DC. *Ford et al.* [2009] employed a grid search with inverse square-root distance weighting, whereas this study uses a DC solution drawn from the millions of full moment tensor solutions that comprise the NSS with inverse distance weighting and down-weighting the of distant stations, HIA and BJT, by a factor of two. With the use of the NSS now all solutions are fit in the same manner and there is no need to use constrained inversions or grid searches to find other than full moment tensor solutions for comparison.

The theoretical teleseismic-P of these sources are shown in Figure 2b. The Full and Explosion sources are consistent with the observed array beam shown in black, but the Dev and DC2 sources produce a teleseismic-*P* that is anti-correlated with the data. The $CC_{\text{Tele-P}}$ for these sources are given in Table 1. As described in equation (5), since the $CC_{\text{Tele-P}}$ are negative for the Dev and DC2 sources, the new *VR* for these sources is set to zero, whereas the new *VR* for the Full and Explosion sources are the same as the *VR* calculated with the regional data (VR_{Reg}) since $CC_{\text{Tele-P}}$ is positive for these sources. The source DC1 with waveforms given in green is an example of a source that fits the teleseismic-*P* data and has a positive $CC_{\text{Tele-P}}$ but is anti-correlated with the regional data with a VR_{Reg} of −90%. In this case, according to equation (5), the *VR* is carried through to the new NSS, but retains the negative *VR*.

The teleseismic-P constraint could contribute more information on the radiation pattern than is provided in the binary approach given by equation (5). However, this simple approach results in a strong constraint, and avoids the sometimes difficult calibration of beamformed teleseismic-P amplitudes. An advantage of using array-derived teleseismic-P is the ability to observe low-magnitude events so that the regional analysis is not limited. For example, the m_b3.9 2006 DPRK nuclear test was at the limit of intermediate-period analysis recorded by a sparse network at far-regional distances [*Ford et al.*, 2010], but teleseismic-P from the event was clearly observed at many arrays [*Selby*, 2010].

4. Conclusions

The Network Sensitivity Solution (NSS) using regional (Δ<13°) intermediate-period (T>10s) full-waveforms introduced in *Ford et al.* [2010] is improved with the use of array-based telseismic-P (Δ>30°) observations. The standard NSS, which calculates the goodness-of-fit of the data to a uniform distribution of all sources and contours the fit on the source-typle plot of *Hudson et al.* [1989], is modified so that the goodness-of-fit for sources that predict teleseismic-*P* which are anti-correlated with array-based observations is set to zero. We apply this constraint to the NSS of the 2009 Memorial Day explosion in the DPRK and find that it eliminates the trade-off between a shallow explosion and shallow volume-compensated linear-vector dipole with a vertical axis in compression (VCLVD-P). These sources produce similar intermediate-period full waveforms at regional stations that

complicate discrimination. The combined regional and teleseismic approach described here can increase confidence in event discrimination using seismic moment tensors.

Data and Resources

All regional waveforms and data for the arrays, ASAR and NVAR, were obtained from the Incorporated Research Institutions for Seismology (IRIS) Data Management Center (DMC; last accessed 10 April 2011). Array waveforms from GERES were obtained via Automatic Data Request Manager (AutoDRM) running at the Seismological Observatory Graefenberg, Erlangen, Germany (last accessed 1 May 2011). Some plots were made using the Generic Mapping Tools version 4.2.2 (www.soest.hawaii.edu/gmt; Wessel and Smith, 1998; last accessed 10 September 2002).

Acknowledgements

The approach described here arose from conversations with Howard Patton at the 31st Monitoring Research Review in Tucson, Arizona and was motivated by a comment from Thorne Lay at the January 2011 Seismic Review Panel at Patrick Air Force Base, Florida. The array beamforming was done with KBALAP and we thank Doug Dodge for its development. DSD acknowledges AFRL grant FA9453-10-C-0263. This work performed under the auspices of the U.S. Department of Energy by Lawrence Livermore National Laboratory under Contract DE-AC52-07NA27344.

References

Bowers, D. (1997). The October 30, 1994, seismic disturbance in South Africa: Earthquake or large rock burst?, J. Geophys. Res., 102(B5), 9843-57.

Bowers, D. and W. R. Walter (2002). Discriminating between large mine collapses and explosions using teleseismic *P* waves, Pure Appl. Geophys., 159, 803-30.

Burdick, L. J., T. Wallace, and T. Lay (1984). Modeling near-field and teleseismic observations from the Amchitka Test Site, J. Geophys. Res. 89(B6), 4373-88.

Butler, R. and L. Ruff (1980). Teleseismic short-period amplitudes: Source and receiver variations, Bull. Seis. Soc. Amer. 70(3), 831-50.

Clark, R. A. and R. G. Pearce (1988). Identification of multiple underground explosions using the relative amplitude method, Bull. Seis. Soc. Amer. 78(2), 885-97.

Cormier, V. F. (1987). Focusing and defocusing of teleseismic P waves by known three-dimensional structure beneath Pahute Mesa, Nevada Test Site, Bull. Seis. Soc. Amer., 77(5), 1688-1703.

Der, Z. A. and Lees, A. C. (1985). Methodologies for estimating t*(f) from short-period body waves and regional variations of t*(f) in the United States. Geophysical Journal of the Royal Astronomical Society, 82: 125–140. doi: 10.1111/j.1365-246X.1985.tb05131.x

Douglas, A. (1992). *Q* for short-period *P*-waves: is it frequency dependent?, Geophys. J. Int. 108, 110-24.

Douglas, A. (1993). Reply to comment by J. R. Murphy on '*Q* for short-period *P* waves: is it frequency dependent?' by A. Douglas, Geophys. J. Int. 113, 541-42.

Ford, S. R. D. S. Dreger, and W. R. Walter (2009). Source analysis of the Memorial Day explosion, Kimchaek, North Korea, Geophys. Res. Lett., 36(L21304), doi:10.1029/2009GL040003.

Ford, S. R., D. S. Dreger, and W. R. Walter (2010). Network sensitivity solutions for regional moment-tensor inversions, Bull. Seis. Soc., 100(5A), 1962-70, doi: 10.1785/0120090140.

Harjes, H.P. (1990), Design and siting of a new regional array in central Europe: Bull. Seism. Soc. Am., 80, B, 1801-1817.

Herrmann, R. B. (2002). Computer programs in seismology, St. Louis University. www.eas.slu.edu/Earthquake_Center/CPS/

Herrmann, R. B. and K. Hutchenson (1993). Quantification of M_{Lg} for small explosion, Tech. rep., Phillips Laboratory Report PL-TR-93-2070.

Hudson, J. A. (1969). A quantitative evaluation of seismic signals at teleseismic distances - II. Body waves and surface waves from an extended source, Geophys. J. Roy. astr. Soc. 18, 353-370.

Hudson, J. A., R. G. Pearce, and R. M. Rogers (1989). Source type plot for inversion of the moment tensor, J. Geophys. Res., 94, 765–774, doi:10.1029/JB094iB01p00765.

Minson, S., and D. Dreger (2007). Stable inversions for complete moment tensors, Geophys J. Int., 174, 585–592, doi:10.1111/j.1365-246X.2008.03797.x.

Murphy, J. R. (1993). Comment on '*Q* for short-period *P* waves: is it frequency dependent?' by A. Douglas, Geophys. J. Int. 113, 535-40.

Ni, S., D. Helmberger, and A. Pitarka (2010). Rapid source estimation from global calibrated paths, Seis. Res. Lett., 81(3), 498-504, doi: 10.1785/gssrl.81.3.498.

Pearce, R. G., J. A. Hudson, and A. Douglas (1988). On the use of P-wave seismograms to identify a double-couple source, Bull. Seis. Soc. Amer. 78(2), 651-71.

Rogers, R. M. and R. G. Pearce (1992). Use of relative amplitude method to compute "best-fit" earthquake moment tensors, J. Geophys. Res., 97(B10), 14083-95.

Rost, S. and C. Thomas (2002). Array seismology: Methods and applications, Rev. Geophys., 40(3), doi: 10.1029/2000RG000100.

Saikia, C. K. (1994). Modified frequency-wavenumber algorithm for regional seismograms using Filon's quadrature; modelling of Lg waves in Eastern North America, Geophys. J. Int., 118(1), 142-158.

Selby, N. (2010). Relative locations of the October 2006 and May 2009 DPRK announced nuclear tests using International Monitoring System seismometer arrays, Bull. Seis. Soc., 100(4), 1779-84, doi: 10.1785/0120100006.

Tables

Table 1. NSS values

Model	VR_{Reg}	$CC_{\mathrm{Tele\text{-}P}}$	VR
Full	81	0.77	81
Dev	80	−0.66	0
DC1	−90	0.82	−90
DC2	72	−0.52	0
Explosion	75	0.77	75

Figures

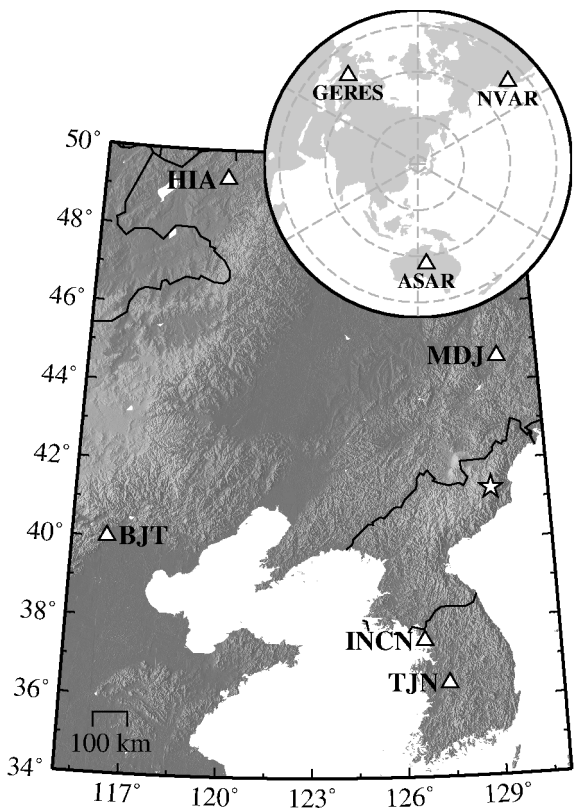

Figure 1. Map of the Yellow Sea/Korean Peninsula with the 2009 Memorial Day explosion (star) as well as the regional stations used in the analysis (triangles). Inset, azimuthal equidistant map of teleseimic arrays used in the analysis (triangles), where the origin is the location of the explosion.

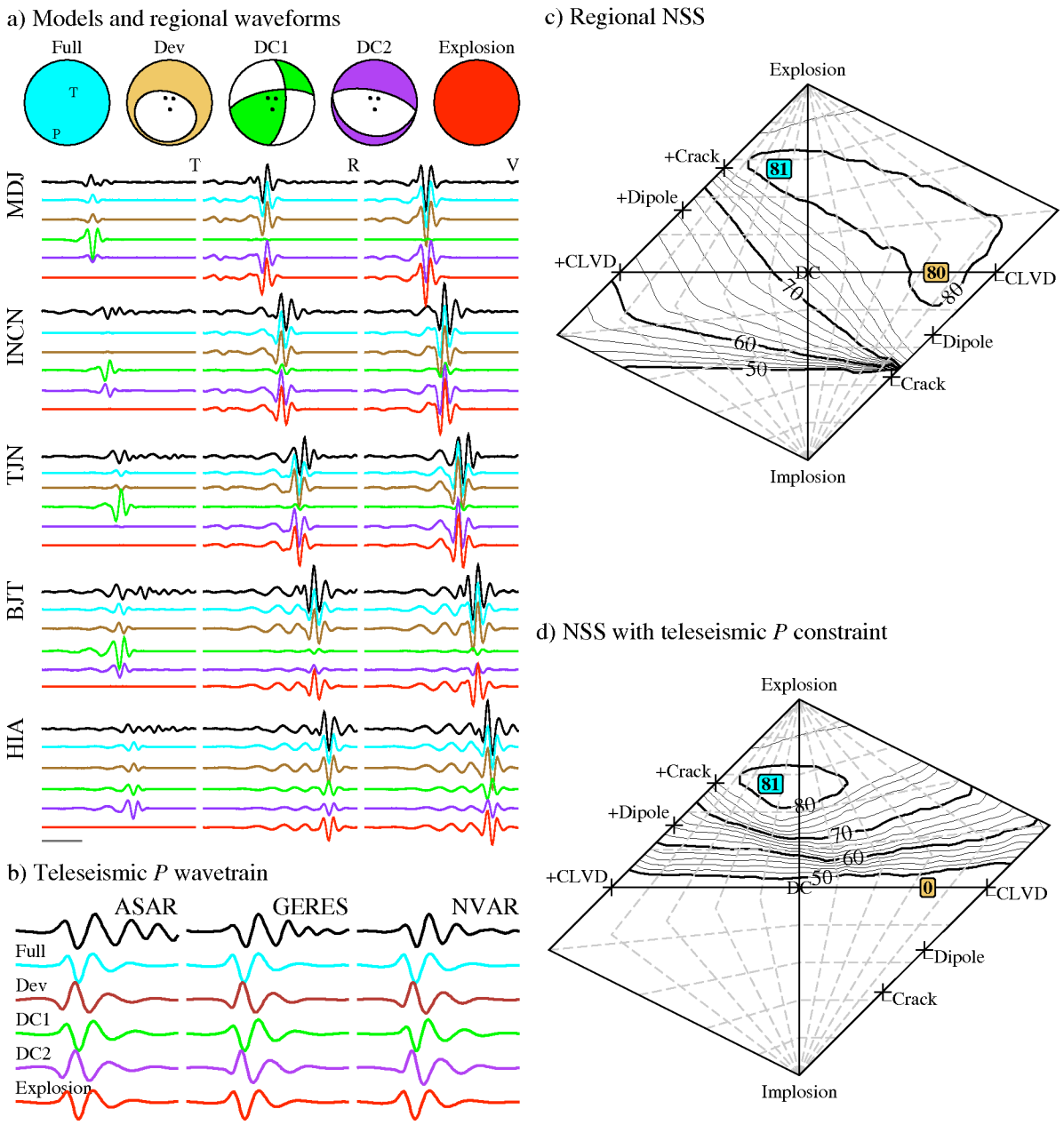

Figure 2. Teleseismic constraint to regional source-type determination. a) Three-component (Tangential, Radial, and Vertical) intermediate period (10-50s) displacements (black) from regional stations shown in Figure 1 and synthetic waveforms at those stations predicted by the sources shown with a lower-hemisphere equal-area focal-sphere. Amplitudes are normalized to the maximum of the three components at each station. The gray bar is 50 sec long. The color of the predicted waveform matches the color of the compressional component of the focal-sphere. The T and P axes are plotted on the focal-sphere of the best-fit full moment-tensor (Full). The ak135-predicted take-off angles to the teleseismic stations shown in Figure 1 are given by the small circles on the focal-spheres of the best-fit deviatoric (Dev), and two examples of double-couple solutions (DC1 and DC2). For comparison, the best-fit explosion is also given (Explosion). b) Array beams of high-

frequency (0.8-4.5 Hz) teleseismic-P wavetrains (black) at the arrays shown in Figure 1, and synthetic waveforms at those arrays predicted by the sources given in a). Each trace is 4 sec long. The color of the predicted waveform matches the color of the compressional component of the focal-sphere. Note the anticorrelation of the teleseismic P predicted by the best-fit full and deviatoric (Dev) sources. c) Contours of fit (Variance Reduction, VR) to the regional data shown in a) for a uniform distribution of sources on the source-type plot. This Network Sensitivity Solution (NSS) shows comparable fit to the data for a CLVD-like source (Dev) and an explosion-like source (Full) with a similar VR of 80% versus 81%, respectively. This trade-off is due to the shallow source recorded by surface stations using intermediate-period data (an explosion in this passband 'looks' like a shallow CLVD at regional stations). d) The NSS given in c) but where the VR is now zero if the teleseismic-P and forward-predicted synthetic data are anticorrelated, as is the case for the deviatoric source (Dev).